Microbiological Research 168 (2013) 367–378

Contents lists available at SciVerse ScienceDirect

Microbiological Research

journal homepage: www.elsevier.com/locate/micres

Biochemical characteristic of biofilm of uropathogenic *Escherichia coli* Dr$^+$ strains

Beata Zalewska-Piątek[a,*], Sabina Wilkanowicz[a], Piotr Bruździak[b], Rafał Piątek[a], Józef Kur[a]

[a] Department of Microbiology, Gdańsk University of Technology, ul. G. Narutowicza 11/12, 80-233 Gdańsk, Poland
[b] Department of Physical Chemistry, Gdańsk University of Technology, ul. G. Narutowicza 11/12, 80-233 Gdańsk, Poland

ARTICLE INFO

Article history:
Received 9 November 2012
Received in revised form
21 December 2012
Accepted 2 January 2013
Available online 30 January 2013

Keywords:
E. coli Dr$^+$
Biofilm
ATR/FTIR-spectroscopy
Dr fimbriae
DraD protein

ABSTRACT

Urinary tract infections caused by *Escherichia coli* are very common health problem in the developed countries. The virulence of the uropathogenic *E. coli* Dr$^+$ IH11128 is determined by Dr fimbriae, which are homopolymeric structures composed of DraE subunits with the DraD protein capping the fiber. In this study, we have analyzed the structural and biochemical properties of biofilms developed by *E. coli* strains expressing Dr fimbriae with or without the DraD tip subunit and the surface-exposed DraD protein. We have also demonstrated that these *E. coli* strains form biofilms on an abiotic surface in a nutrient-dependent fashion. We present evidence that Dr fimbriae are necessary during the first stage of bacterial interaction with the abiotic surface. In addition, we reveal that the DraD alone is also sufficient for the initial surface attachment at an even higher level than Dr fimbriae and that chloramphenicol is able to reduce the normal attachment of the analyzed *E. coli*. The action of chloramphenicol also shows that protein synthesis is required for the early events of biofilm formation. Additionally, we have identified reduced exopolysaccharide coverage in *E. coli* that express only Dr fimbrial polyadhesins at the cell surface with or without the DraD capping subunit.

1. Introduction

Urinary tract infections (UTI) involving the bladder (cystitis) and kidneys (pyelonephritis) are the most common bacterial diseases in humans. *Escherichia coli* is the most frequent agent (about 80%) of UTI in humans and one of the most common causes of gram-negative bacteremia in hospitalized patients (Foxman 2002).

Uropathogenic *E. coli* (UPEC) harbors several urovirulence factors required for adhesion, colonization of host mucosal surfaces, invasion of host cells and tissues, overcoming host defense mechanisms, and persistence. Virulence determinants associated with UPEC include surface factors (S and F1C fimbriae, Dr family of adhesins, and P and type 1 pili) and exported factors (toxins, siderophores, and polysaccharide coatings) (Oelschlaeger et al. 2002; Emödy et al. 2003; Arisoy et al. 2006; Yamamoto 2007). Biofilm formation can be considered as another urovirulence determinant responsible for the long-lasting persistence of bacteria in the genitourinary tract (Costerton et al. 1995).

The Dr family of adhesins, including Dr haemagglutinin (DraE), Dr-II (DraE-II), F1845 (DaaE), Afa-I, Afa-II, Afa-III, Afa-V, Afa-VII, Afa-VIII, Nfa-I, Aaf-I, and Aaf-II (of human or animal origin), are the third most common group of virulence factors characteristic of UPEC, after type 1 and P pili (Nowicki et al. 2001; Van Loy et al. 2002a; Servin 2005; Le Bouguénec and Servin 2006).

Dr haemagglutinin, like the rest of the Dr adhesin family, is encoded by the *dra* gene operon with a similar genetic organization (Nowicki et al. 1989). The Dr adhesin can use up to 4 receptors, such as decay-accelerating factor (DAF) (Nowicki et al. 1988; Carnoy and Moseley 1997; Van Loy et al. 2002a,b; Korotkova et al. 2008a), members of the carcinoembryonic antigen family (CEA; Berger et al. 2004; Korotkova et al. 2008a,b; Guignot et al. 2009), type IV collagen, and $\alpha_5\beta_1$ integrin, to adhere to host cells and tissues (Westerlund et al., 1989; Carnoy and Moseley, 1997; Guignot et al. 2009). The adherence phenotype of *E. coli* Dr$^+$ strains is responsible for bacterial aggregation, which is the first step of biofilm formation (Zalewska-Piątek et al. 2008, 2009).

A bacterial biofilm is defined as a three-dimensional structured community of aggregated cells embedded in a self-produced exopolysaccharide matrix that is able to adhere to abiotic and living (biotic) surfaces. Many persistent and chronic bacterial infections are believed to be associated with biofilm formation (Costerton et al. 1995, 1999). Pathogenic bacteria that form biofilms can be up to 1000 times more resistant to antimicrobial agents, such as antibiotics, and host immune attacks (Anderson and O'Toole 2008; Stewart and Franklin 2008). The ability of bacterial cells to develop biofilms is not only responsible for many health problems but also causes economic losses (Costerton et al. 1999).

Biofilms are created by many punctate microcolonies that are separated by water-filled channels used for supplying nutrients and removing waste products and are surrounded by an exopolysaccharide coverage. Exopolysaccharide production is not required for surface attachment but for the development of the

* Corresponding author. Tel.: +48 58 3471862.
E-mail address: beazalew@pg.gda.pl (B. Zalewska-Piątek).

0944-5013/$ – see front matter © 2013 Elsevier GmbH. All rights reserved.
http://dx.doi.org/10.1016/j.micres.2013.01.001

Table 1
E. coli strains and plasmids.

E. coli strain	Mutation	Relevant genotype				Surface exposure of		Source/reference
		draC	*draD*	*draE*	*gspD*	DraD	DraE	
BL21(DE3)	*ompT lon dcm*	–	–	–	+	–	–	Novagen
BL21(DE3)/pCC90	–	+	+	+	+	+	+	Carnoy and Moseley (1997)
BL21(DE3)/pCC90DraDmut	Δ*draD*stop	+	–	+	+	–	+	Zalewska et al. (2005)
BL21(DE3)/pCC90DraCmut	DraC–K15stop	–	+	+	+	+	–	Zalewska et al. (2005)
BL21(DE3)/pCC90D54stop	Dr-D54stop	+	+	–	+	+	–	Carnoy and Moseley (1997)
DR14/*gspD*	Insertion DraC, intron GspD	–	+	+	–	–	–	Zalewska-Piątek et al. (2008)
IH11128	–	+	+	+	+	+	+	Nowicki et al. (1987)
DR14	Insertion DraC	–	+	+	+	+	–	Goluszko et al. (1997)

three-dimensional architecture of *E. coli* biofilms (Costerton et al. 1994, 1995; Danese et al. 2000; Prigent-Combaret et al. 2001).

Biofilm development can be divided into the following steps. The first step includes the sedimentation of planktonic cells on the biotic or abiotic surfaces, adhesion, and creation of a cluster. The second step involves the formation of antimicrobial-resistant colonies. Further steps are connected with the removal of individual cells from the biofilm colonies, their settling on a surface, and the creation of new agglomerations (Costerton et al. 1994, 1995).

Biofilm formation is strongly influenced by nutritional conditions (Costerton et al. 1995; Terada et al. 2003), ionic strength (Busalmen and de Sánchez 2001; Gomez et al. 2003), and osmotic pressure (Prigent-Combaret et al. 2001; Kawarai et al. 2009). An increase in osmolarity of up to 0.3 M NaCl in the culture medium inhibited biofilm formation by *E. coli* (Prigent-Combaret et al. 2001) and slowed the growth of the analyzed bacteria (Record et al. 1998).

Here, we studied for the first time the structural (distribution of the polysaccharide matrix and content of proteins and phosphates) and biochemical properties of biofilms formed by strains of *E. coli* harboring the *dra* gene cluster. The investigations were concentrated on *E. coli* strains of laboratory and clinical origin that expressed Dr fimbriae with or without DraD as a capping fimbrial subunit, the so-called fimbria-associated form ($DraD^+/DraE^+$ and $DraD^-/DraE^+$, respectively), and the DraD protein as a fimbria non-associated structure ($DraD^+/DraE^-$). The results obtained will form the background for future studies on the development of biofilms of *E. coli* Dr^+ strains. We investigated the effect of various nutrients and a highly osmotic environment on *E. coli* biofilm development. We found that biofilm formation by *E. coli* Dr^+ strains can be inhibited in the presence of the protein synthesis inhibitor chloramphenicol (CLM), which can also abolish the adhesion mediated by Dr haemagglutinin (a phenotype critical for attachment to abiotic surfaces). In addition, we found that the exopolysaccharide matrix of *E. coli* strains exposing Dr fimbriae with ($DraD^+/DraE^+$) or without ($DraD^-/DraE^+$) the DraD tip subunit was less intensely stained with periodic acid-Schiff (PAS) reagent (reduced exopolysaccharide coverage) than were biofilm polysaccharides surrounding subpopulations of *E. coli* in which the DraD protein was not associated with fimbriae ($DraD^+/DraE^-$) (increased exopolysaccharide coverage). Finally, we characterized the chemical structure of biofilms colonizing abiotic surfaces by using attenuated total reflection Fourier transform infrared spectroscopy (ATR/FTIR). The difference spectra displayed features originating from various biopolymers specific to the *E. coli* strains that formed the biofilms.

2. Materials and methods

2.1. Bacterial strains, plasmids, and reagents

The strains used in this study are described in Table 1. The overexpression of genes encoded by a *dra* gene cluster was performed in the laboratory *Escherichia coli* strain BL21(DE3) (Novagen, Nottingham, UK) or the clinical *E. coli* strains IH11128 (Nowicki et al. 1987), DR14 (Goluszko et al. 1997), and DR14/*gspD* (Zalewska-Piątek et al. 2008).

E. coli BL21(DE3) is a λDE3 strain carrying the gene for T7 polymerase that is under the control of the *lacUV5* promoter. *E. coli* IH11128 is a strain of clinical origin (isolated from a patient with pyelonephritis) with Dr fimbriae (Nowicki et al. 1987). *E. coli* DR14 is an insertional *draC* mutant strain (Goluszko et al. 1997). The *E. coli* DR14/*gspD* strain is a *gspD* mutant (with a *gspD* gene knockout) of *E. coli* DR14 that was described previously (Zalewska-Piątek et al. 2008).

The plasmids pCC90 carrying the *dra* gene cluster with its promoter region (*draF-draA*) upstream of a deleted *draB* gene, and pCC90D54stop, a DraE-negative mutant (with the mutated *draE* gene), were provided by S. Moseley, University of Washington, Seattle, WA, USA (Carnoy and Moseley 1997). The plasmids pCC90DraDmut, a DraD-negative mutant (with the mutated *draD* gene), and pCC90DraCmut, a DraC-negative mutant (with the mutated *draC* gene), have been described previously (Zalewska et al. 2005).

Bacterial *E. coli* strains (of laboratory or clinical origin) were grown on rich medium (Luria-Bertani [LB]) or minimal medium (M63) (as indicated in each experiment), supplemented with the appropriate antibiotic (100 μg ampicillin ml^{-1}) (Sigma, St. Louis, MO), at 37 °C.

Polyvinylchloride ([PVC]; 96-well, microtest flexible assay plates) or polystyrene plates (6-well flexible assay plates) and glass coverslips were obtained from Becton Dickinson (Franklin Lakes, NJ). One percent crystal violet (CV), a dye used for staining attached cells but not PVC, was purchased from Merck (Darmstadt, Germany).

2.2. Cell lines

HeLa cells were maintained on minimum essential medium (MEM) supplemented with 10% (v/v) fetal bovine serum (FBS; Sigma) and penicillin–streptomycin solution (Sigma) in a 5% CO_2 atmosphere at 37 °C. The cell line was passaged using 0.25% (v/v) trypsin containing EDTA (Sigma).

2.3. Growth of biofilms under different nutritional environments

Biofilm formation was assayed using the ability of bacterial cells of laboratory and clinical origin (grown on minimal medium) to adhere to the wells of 96-well microtiter plates made of PVC, as described previously (Zalewska-Piątek et al. 2009). The minimal medium used was M63 supplemented with glucose (0.2%); glucose (0.2%) plus $FeSO_4$ (3 μM); glucose (0.8%) plus LB (1%); and casamino acids (CAA, 1%). After 24 h of static growth (37 °C) in the wells of the plates, the biofilms formed from M63-grown cells were stained with 1% (w/v) CV, and the absorbance was determined at 531 nm (Victor3V plate reader; PerkinElmer, Waltham,

MA) (Zalewska-Piątek et al. 2009). Strains showing a blank corrected mean absorbance value of >0.1 were considered positive.

2.4. Biofilm formation under high osmotic pressure

Biofilm formation on the wells of 6-well polystyrene plates supported with the glass coverslips was studied. Control LB medium, LB without sodium chloride (LB-WS; 1% tryptone and 0.5% yeast extract) (Kawarai et al. 2009), and LB-WS supplemented with 1 M sodium chloride (LB-WSN) or sucrose (LB-WSS; Sigma) were used in the experiments. The 24-h cell cultures grown under static conditions were diluted in fresh media (1:100) and grown statically for another 24 h, at 37 °C, in the wells of microtiter plates. The glass slides were then rinsed three times with deionized water, dried for 30 min at room temperature, and Gram-stained. Biofilms formed on glass slides after Gram staining were observed using light microscopy with a 40× objective lens and an Olympus BX60 microscope (Olympus, Tokyo, Japan). ImageJ software was used for image analysis and processing.

The second 96-well PVC microtiter plate, stained with 1% (w/v) CV (Zalewska-Piątek et al. 2009) was used for the quantitative analysis of biofilm formation under high osmotic pressure in an environment of 1 M NaCl or 1 M sucrose. The absorbance was determined at 531 nm (Victor 3V plate reader; PerkinElmer). Strains presenting a blank corrected mean absorbance value of >0.1 were considered positive.

2.5. Effect of chloramphenicol inhibition on biofilm formation

Bacterial strains were grown statically for 24 h in M63 with 0.2% glucose and 1% LB at 37 °C. Subsequently, the cells were subcultured (1:40 dilution) into fresh media, in the presence or absence of 3.5 mM CLM (Sigma), for another 24 h of static growth at 37 °C in the wells of PVC microtiter plate. After 24 h, the wells were rinsed and the biofilms stained with 1% CV. Then, the A_{531} of each CV sample was determined using the Victor 3V plate reader (PerkinElmer). Strains presenting a blank corrected mean absorbance value of >0.1 were considered positive.

2.6. Effect of chloramphenicol on bacterial binding to HeLa cells

HeLa cells were split into 12-well plates with glass coverslips and grown for 24 h. Before the assay, the cells were washed twice with MEM and incubated in fresh medium without antibiotics and FBS for 1 h. The bacterial strains were grown overnight in M63 with 0.2% glucose and 1% LB. The cells were then pelleted and resuspended in PBS (OD_{595}, 0.8). 50 μl of each bacterial strain suspension was added to the wells of the plate, together with 50 μl of PBS containing 0.2% BSA and 3.5 mM CLM, and incubated for 1.5 h at 37 °C with 5% CO_2 (the control experiment was conducted without CLM bacterial inhibitor). After incubation, the cells were stained with Giemsa and analyzed, as reported previously (Zalewska-Piątek et al. 2008).

2.7. Exopolysaccharide periodic acid-Schiff staining

Biofilms were cultivated in M63 with 0.2% glucose and 1% LB in 6-well plates on glass coverslips. After fixation of the bacterial cells in 10% neutral-buffered formalin, the exopolysaccharide coverage of 24-h biofilms was determined by PAS-staining (Sigma), according to the manufacturer's instructions. Following this, the coverslips were rinsed with deionized water, air dried, and examined microscopically under a 40× objective lens (Olympus CKX41). The images were analyzed by using Kodak ST34 Scanner Step Tablet which allows for the conversion of pixel values to optical density (OD) units.

2.8. Evaluation of the biofilms by using ATR/FTIR

Overnight static bacterial cell cultures were diluted (1:40) in fresh M63 medium with 0.2% glucose and 1% LB and grown statically in 96-well PVC microtiter plates for another 24 h, at 37 °C. After 24 h, the plates were purged twice with PBS and left to dry at room temperature. At least 5 wells were prepared for every strain. To measure the spectrum of the biofilm, the bottom of each air-dried well was cut out by using a sharp cork borer and pressed to the surface of the diamond crystal of the ATR accessory.

The FTIR spectra of biofilm samples were measured using an FTIR spectrometer (Nicolet 8700; Thermo Electron Corp., Waltham, MA) equipped with the GoldenGate (Specac Corp., Oprington, UK) ATR accessory with a single reflection diamond crystal. The temperature of the crystal was maintained at 25.0 ± 0.1 °C by using an automatic temperature controller (Specac Corp.) coupled with the ATR accessory. In each measurement, 64 scans were collected with a resolution of 4 cm^{-1} and in the range of 2000–550 cm^{-1}. The spectrum of the PVC material of the plate was measured and later subtracted from every measured spectrum as the background. After measuring all FTIR spectra corresponding to a selected strain and background subtraction, the average spectrum was calculated. The spectrometer was purged with dry nitrogen to diminish the negative influence of water vapor.

3. Results

3.1. Effects of nutritional environment and osmolarity on E. coli biofilm formation

The nutritional environment can strongly influence biofilm development (Costerton et al. 1995; Wimpenny and Colasanti 1997). Therefore, we tested the effect of various nutrients that supplement minimal M63-based media on the ability of the laboratory *E. coli* strains BL21(DE3) (Fig. 1A), BL21(DE3)/pCC90 (Fig. 1B), BL21(DE3)/pCC90DraDmut (Fig. 1C), BL21(DE3)/pCC90DraCmut (Fig. 1D), and BL21(DE3)/pCC90D54stop (Fig. 1E) and the clinical *E. coli* strains DR14/*gspD* (Fig. 1F), IH11128 (Fig. 1G), and DR14 (Fig. 1H) to form biofilms on PVC plates. All strains of *E. coli dra*$^+$ showed normal and equal growth in M63 medium, regardless of the nutrients added to the medium (see the growth curve in Fig. 1). Therefore, in order simplify the image in Fig. 1, the presented graph shows a single growth curve corresponding to all *E. coli* strains and one for the analyzed M63 media. In M63 medium, without any nutritional supplementation and after a 2-h period of growth, slow growth of all bacterial *E. coli* strains was observed up to OD_{595} = 0.08, and the increase in absorbance and culture growth subsequently ceased.

Biofilm formation was visualized with CV staining after 48 h of static growth. Biofilm development was effectively supported by glucose (as a carbon and energy source)/iron, glucose/LB, and CAA in almost all the analyzed *E. coli* strains containing the *dra* gene cluster and also in mutants showing inactivation of the *draD* gene (with surface presentation of Dr fimbriae) or the *draE* and *draC* genes (exposing only DraD at the cell surface in a fimbria non-associated form). The increased effect of biofilm formation (by approximately 4- to 6-fold) was observed especially in the case of the laboratory *E. coli* strains BL21(DE3)/pCC90 (Fig. 1B), BL21(DE3)/pCC90DraCmut (Fig. 1D), and BL21(DE3)/pCC90D54stop (Fig. 1E) and the clinical *E. coli* strain IH11128 (Fig. 1G). Other strains of *E. coli* developed biofilms at comparable levels in all types of media used, regardless of nutrient

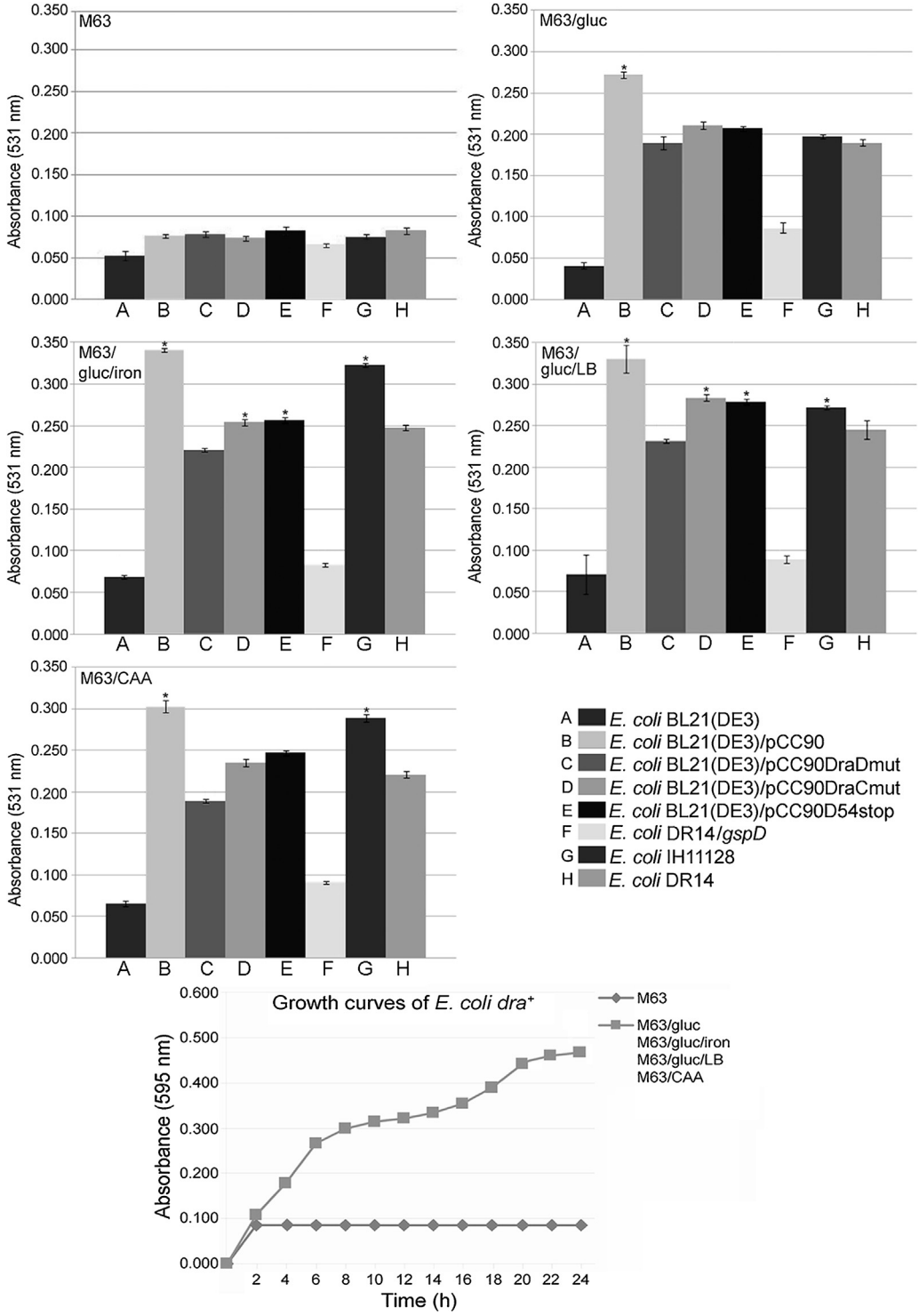

Fig. 1. Nutritional effect on biofilm development by *E. coli dra*$^+$ strains. The biofilm formation phenotype was assayed with bacterial cells grown on minimal M63 medium supplemented with glucose, glucose plus iron, glucose plus LB, and CAA (A to H). *E. coli* strains were stained with CV and the A_{531} of each CV sample was determined. (A) *E. coli* BL21(DE3), (B) *E. coli* BL21(DE3)/pCC90, (C) *E. coli* BL21(DE3)/pCC90DraDmut, (D) *E. coli* BL21(DE3)/pCC90DraCmut, (E) *E. coli* BL21(DE3)/pCC90D54stop, (F) *E. coli* DR14/*gspD*, (G) *E. coli* IH11128, and (H) *E. coli* DR14. Each bar represents the mean ± SEM from 3 independent experiments. The graph represents a growth curve that is representative of all *E. coli* strains and of the analyzed M63 media. Statistical analysis was performed using Student's *t* test. Asterisks indicate statistically significant differences ($P < 0.05$ for each strain). The significance was calculated for the difference between A and B, C, D, E, F, G, and H.

supplementation. The minimal M63 media without the addition of glucose, CAA, and an iron source did not promote biofilm development, as assayed by CV staining. The strains *E. coli* BL21(DE3) and DR14/*gspD* (with the *draC* and *gspD* gene knockout; Fig. 1A and F, respectively) were defective in forming biofilms independent of the nutritional environment.

We also determined the role of osmotic pressure on biofilm formation by the *E. coli dra*$^+$ strains on polystyrene plates by using 2 osmolytes, NaCl and sucrose, to mimic the conditions of high osmolarity found in the urinary tract (Brauner et al. 1990). The effect of osmolarity was analyzed in LB-WS (Fig. 2B, F, J, M, and R) supplemented with NaCl (LB-WSN; Fig. 2C, G, K, N and S) or

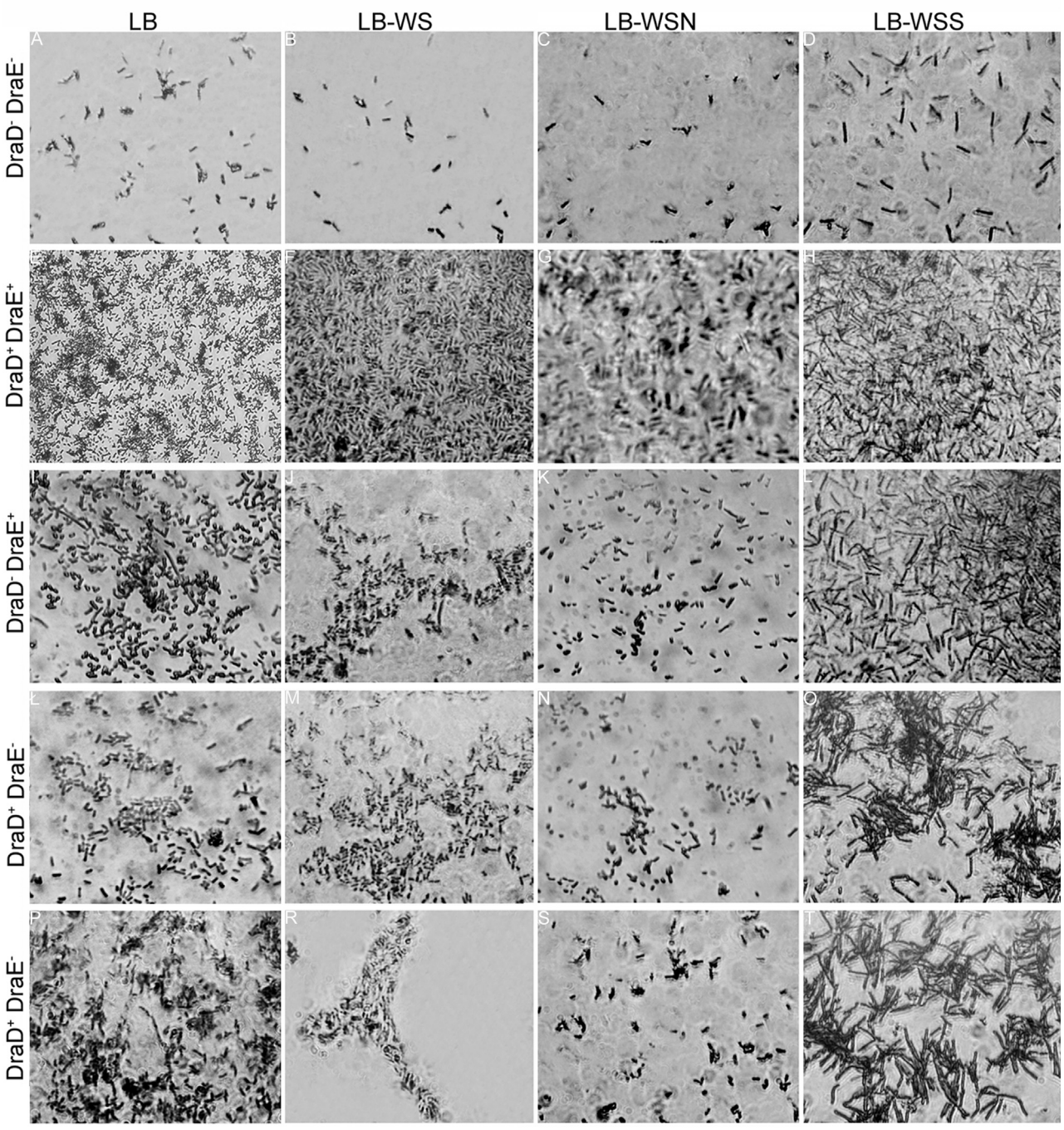

Fig. 2. Effect of osmolarity on biofilm formation by *E. coli dra*$^+$ strains after Gram staining. Biofilm-forming cells on glass slides were grown in LB, LB-WS without sodium chloride, LB-WSN with 1 M sodium chloride, and LB-WSS with 1 M sucrose. *E. coli* strains were Gram-stained and subjected to light microscopy (ME). The same set of *E. coli* strains was used in each experiment with different media. Microscopic examination (ME) of (A, B, C, D) *E. coli* BL21(DE3), (E, F, G, H) *E. coli* BL21(DE3)/pCC90, (I, J, K, L) *E. coli* BL21(DE3)/pCC90DraDmut, (L, M, N, O) *E. coli* BL21(DE3)/pCC90DraCmut, and (P, R, S, T) *E. coli* BL21(DE3)/pCC90D54stop, grown in LB (A, E, I, L, P), LB-WS (B, F, J, M, R), LB-WSN (C, G, K, N, S), or LB-WSS (D, H, L, O, T). Magnification, 4000× (Olympus BX60 microscope).

sucrose (LB-WSS; Fig. 2D, H, L, O, and T) by using only the laboratory *E. coli* strain BL21(DE3), harboring the *dra* gene cluster, following Gram staining (Fig. 2A–T). This approach was closely associated with those of earlier studies that revealed the effect of inhibition on biofilm formation of the clinical *E. coli* IH111128 and DR14 strains (containing the whole *dra* gene cluster with a regulatory *draF-draA* region) cultured in LB medium (Zalewska-Piątek et al. 2009). In 1 M sucrose nutrient broth, growth retardation was observed for all the studied *E. coli dra*$^+$ strains, and the culture turbidity began to increase slowly after 10 h of bacterial growth. The increase in bacterial growth was observed within a 24-h period. The slow growth of bacterial cells had no effect on their ability to form biofilms (Fig. 3). Normal growth was observed in LB and LB-WS media (data not shown). Thick and elongated bacterial cells grown in hypertonic broth containing 1 M sucrose were alive, as evidenced by the observed slow growth increase (observed as a slow increase in absorbance). The higher osmolarity of 1 M NaCl than of 1 M sucrose led to a stronger inhibitory effect on the growth of the

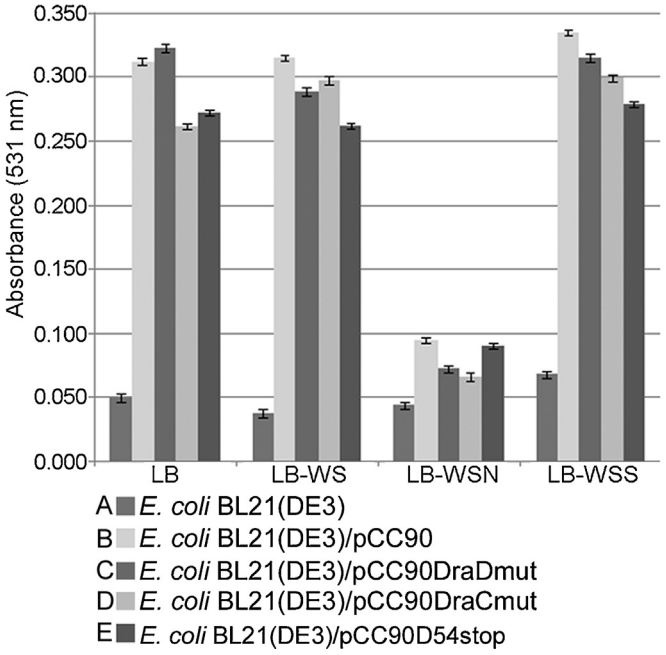

Fig. 3. Effect of osmolarity on biofilm formation by *E. coli dra*$^+$ strains after CV-staining. Biofilm-forming cells on glass slides were grown in LB, LB-WS without sodium chloride, LB-WSN with 1 M sodium chloride, or LB-WSS with 1 M sucrose. Subsequently, the cells were stained with CV and subjected to spectrophotometric measurement at 531 nm. The same set of *E. coli* strains was used in each experiment with different media. Microscopic examination (ME) of (A) *E. coli* BL21(DE3), (B) *E. coli* BL21(DE3)/pCC90, (C) *E. coli* BL21(DE3)/pCC90DraDmut, (D) *E. coli* BL21(DE3)/pCC90DraCmut, and (E) *E. coli* BL21(DE3)/pCC90D54stop. Each bar represents the mean ± SEM from 3 independent experiments.

bacterial cells. A slight growth of bacterial cultures was observed up to OD_{595} = 0.07 within a 3-h period, and then the growth was totally inhibited (data not shown).

In the osmolarity experiments, *E. coli* BL21(DE3) without the genes of the *dra* gene cluster (*dra*$^-$) was used as a negative control for biofilm formation (Fig. 2A–D). The rest of the *E. coli dra*$^+$ strains did not form biofilms in LB-WSN with NaCl at a concentration of 1 M (Fig. 2G, K, N, and S). In contrast, the same *E. coli* strains developed biofilms in LB-WSS with 1 M sucrose (Fig. 2H, L, O, and T). Culture growth retardation was observed only slightly after 24 h, which allowed the execution of the experiments. However, almost all Gram-stained bacterial cells that developed biofilms in the sucrose environment showed a thick and elongated morphology (cell size, 1.5 μm × 10 μm), compared to that of biofilm-forming cells grown on LB (Fig. 2E, I, Ł, and P) or LB-WS media (Fig. 2F, J, M, and R) (cell size, 1 μm × 2 μm). In addition, in the case of the DraD$^+$/DraE$^-$ (pCC90DraCmut and pCC90D54stop) *E. coli* strains (Fig. 2O and T), the bacterial cells formed clusters of higher density than the DraD$^+$/DraE$^+$ (pCC90) (Fig. 2H) and DraD$^-$/DraE$^+$ (pCC90DraDmut) (Fig. 2L) *E. coli* strains. The clusters contained more than 10 cells that were in physical contact. The data obtained were also verified by quantitative analysis of biofilm formation under the high osmotic pressure by CV staining of bacterial cells (on the PVC plates) and spectrophotometric measurement (Fig. 3 A–E). The CV-staining results confirmed the role of Dr fimbriae in the adhesion of *E. coli* Dr$^+$ strains to the abiotic substrates during biofilm development under high osmotic pressure (in LB-WSS medium). Taken together, the data obtained suggest that 1 M sodium chloride that is used to create a highly osmotic environment significantly inhibits biofilm formation by *E. coli dra*$^+$ strains and that the 1 M sucrose environment influences the morphology of biofilm-forming bacterial cells.

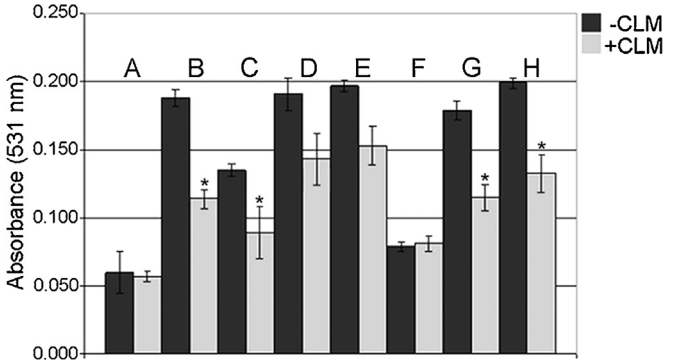

Fig. 4. Effect of CLM activity on biofilm formation by *E. coli dra*$^+$ strains. Bacterial cells were grown in the absence (−CLM) or presence (+CLM) of CLM, stained with CV, and subjected to spectrophotometric measurement at 531 nm. (A) *E. coli* BL21(DE3), (B) *E. coli* BL21(DE3)/pCC90, (C) *E. coli* BL21(DE3)/pCC90DraDmut, (D) *E. coli* BL21(DE3)/pCC90DraCmut, (E) *E. coli* BL21(DE3)/pCC90D54stop, (F) *E. coli* DR14/*gspD*, (G) *E. coli* IH11128, and (H) *E. coli* DR14. Each bar represents the mean ± SEM from 3 independent experiments. Statistical analysis was performed using Student's *t* test. Asterisks indicate statistically significant differences ($P < 0.05$ for each strain).

3.2. Chloramphenicol inhibition of biofilm formation and competition of bacterial adherence

The receptor interactions of DraE adhesin are blocked by the antibiotic CLM. Nowicki et al. (1988) observed that CLM-contaminated reagent completely abolished DAF-mediated mannose-resistant haemagglutination. Further experiments revealed that CLM is also responsible for the inhibition of interactions between type IV collagen and CEA receptor (Westerlund et al. 1989; Korotkova et al. 2006). The normal bacteriostatic activity of CLM is associated with its ability to act as an inhibitor of the 50S prokaryotic ribosome (Moazed and Noller 1987). Besides the toxic effect, in the case of *E. coli* Dr$^+$ strains, CLM plays key role as an inhibitor of Dr adhesion (Pettigrew et al. 2009). The adhesive properties of bacterial cells usually mediate the first step of biofilm development and formation of cell microcolonies (Costerton et al. 1995; Soto et al. 2007).

To test these findings, cells of the laboratory *E. coli* strain BL21(DE3) transformed with pCC90, pCC90DraDmut, pCC90DraCmut, or pCC90D54stop, and those of the clinical *E. coli* strains (IH11128, DR14, and DR14/*gspD*) were incubated in the presence or absence of CLM (a protein synthesis inhibitor) in microtitre wells for 24 h (on the minimal medium supplemented with glucose). Then, the cells were stained with CV to assess biofilm formation. CLM caused no inhibition of bacterial growth within a 24-h period. The growth rate was the same for all the studied *E. coli* strains, regardless of the presence or absence of CLM in the culture medium (data not shown).

As shown in Fig. 4, compared to untreated strains, after 24 h, biofilm formation was inhibited in the presence of CLM, especially in the case of *E. coli* BL21(DE3)/pCC90 (Fig. 4B), *E. coli* IH11128 (Fig. 4G), and *E. coli* BL21(DE3)/pCC90DraDmut (Fig. 4C) bearing Dr fimbriae with or without DraD as a capping fimbrial subunit. Considering that the strains presenting a blank corrected mean absorbance value of >0.1 were regarded as positive, we could conclude that CLM activity almost completely blocked biofilm development by *E. coli* BL21(DE3)/pCC90DraDmut (Fig. 4C). In the case of *E. coli* BL21(DE3)/pCC90 (Fig. 4B) and *E. coli* IH11128 (Fig. 4G), biofilm formation capacity was reduced by over 80%. Other *E. coli* laboratory and clinical strains with only surface-exposed DraD, *E. coli* BL21(DE3)/pCC90DraCmut (Fig. 4D), BL21(DE3)/pCC90D54stop (Fig. 4E), and DR14 (Fig. 4H) revealed 50% and over 65% reduction of biofilm development (in

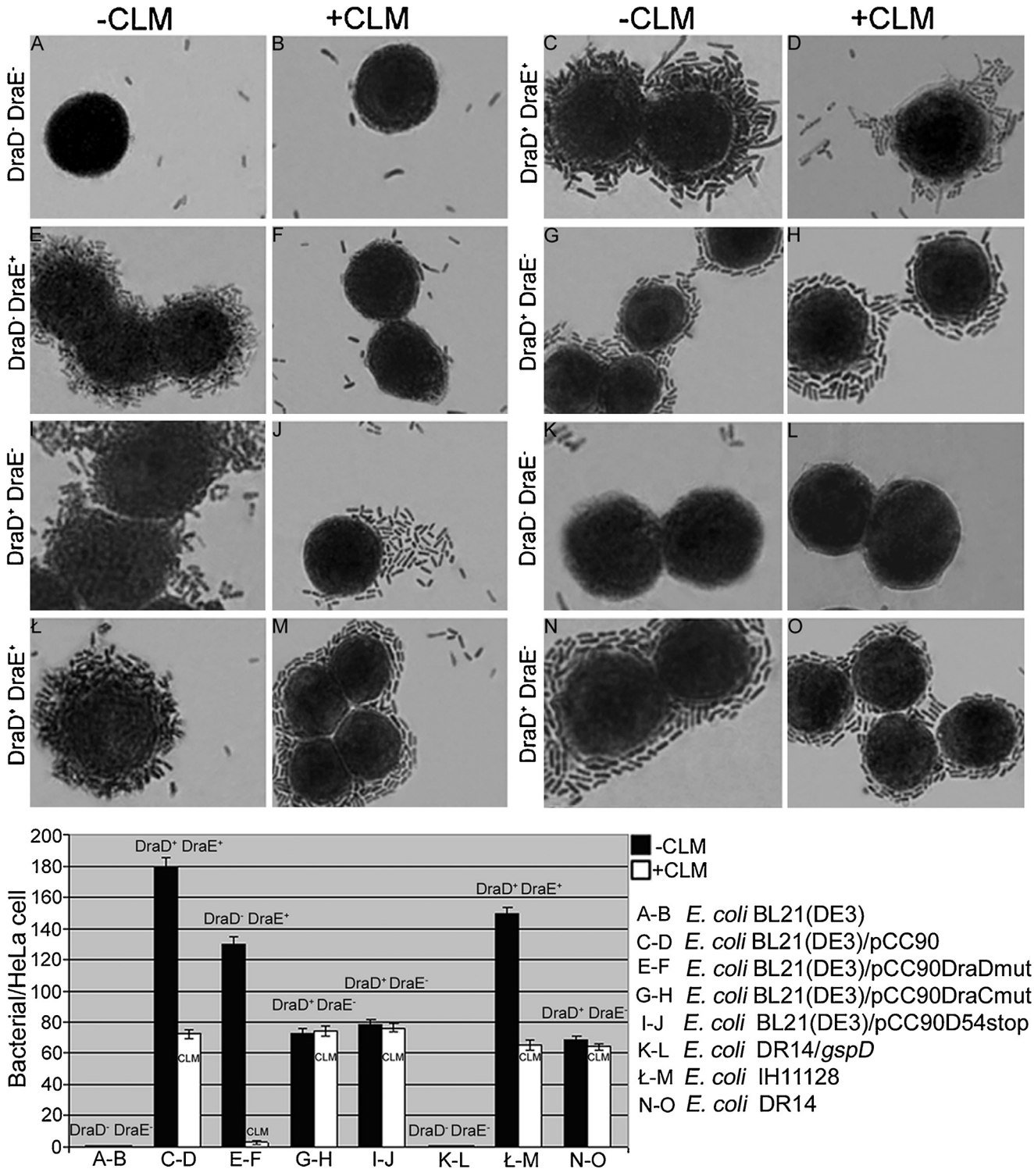

Fig. 5. Adherence of the *E. coli dra*$^+$ strains to HeLa cells. Bacterial strains were bound to HeLa cells in the absence (−CLM) or presence of CLM (+CLM), fixed, stained with Giemsa, and subjected to light microscopy (ME). (A, B) ME of *E. coli* BL21(DE3), (C, D) *E. coli* BL21(DE3)/pCC90, (E, F) *E. coli* BL21(DE3)/pCC90DraDmut, (G, H) *E. coli* BL21(DE3)/pCC90DraCmut, (I, J) *E. coli* BL21(DE3)/pCC90D54stop, (K, L) *E. coli* DR14/*gspD*, (Ł, M) *E. coli* IH11128, and (N, O) *E. coli* DR14. Forty cells associated with bacteria were examined by light microscopy, and the attachment of *E. coli* to HeLa cells was quantified. −CLM (A, C, E, G, I, K, Ł, N); +CLM (B, D, F, H, J, L, M, O). Magnification, 10,000× (Olympus BX60 microscope). Black boxes, adhesion in the absence of CLM. Open boxes, adhesion in the presence of CLM.

comparison to the corresponding strains grown in the absence of CLM), respectively.

The results achieved were compared with the bacterial adherence of the above *E. coli* strains mixed with the antibiotic CLM along with HeLa cells (Fig. 5) expressing the DAF receptor, which is also abundant in the uroepithelium (Medof et al. 1987). All data are presented in reference to the strains of *E. coli* incubated with HeLa cells, without the addition of CLM. A summary of the relationship between the surface exposure of DraD/DraE proteins and the binding phenotype of the analyzed recombinant *E. coli dra*$^+$ strains in the presence and absence of CLM is given in Table 2. The adhesion abilities of bacteria containing

Table 2
Relationship between the surface expression of DraD/DraE and the binding phenotypes of *E. coli dra*$^+$ strains.

E. coli strain	Surface exposure of		Binding phenotype ($^-$CLM)		Binding phenotype ($^+$CLM)	
	DraD	DraE	DraD[a,b]	DraE[b]	DraD[a,b]	DraE[b]
BL21(DE3)	–	–	–	–	–	–
BL21(DE)/pCC90	+	+	sa+	sa+	[c]aa+	[d]–
BL21(DE3)/pCC90DraDmut	–	+	–	sa+	–	[d]–
BL21(DE3)/pCC90DraCmut	+	–	aa+	–	aa+	–
BL21(DE3)/pCC90D54stop	+	–	aa+	–	aa+	–
DR14/*gspD*	–	–	–	–	–	–
IH11128	+	+	sa+	sa+	[c]aa+	[d]–
DR14	+	–	aa+	–	aa+	–

[a] aa, aggregative adhesion of DraD.
[b] sa, strict adhesion of Dr fimbrial structures (with or without the DraD tip subunit) specifically interacting with receptors on HeLa cells.
[c] Transition of adherence phenotype in the presence of CLM (+CLM).
[d] Loss of binding phenotype.

cell surface-exposed Dr fimbriae were strongly abolished by the interaction of CLM with Dr haemagglutinin (as evidenced by the reduced number of bacteria associated with HeLa cells) (Fig. 5D, F and M). We observed that only individual cells (3 ± 1) of the *E. coli* BL21(DE3)/pCC90DraDmut strain with the mutated *draD* gene were attached to HeLa cells (Fig. 5F). The same bacterial strain, when not incubated with CLM, showed a high level of adherence to HeLa cells (average number of bound bacteria, 130 ± 4) (Fig. 5E). In the case of *E. coli* IH11128 and BL21(DE3)/pCC90, after the addition of CLM, the average number of bacteria associated with HeLa cells was reduced from 150 ± 4 (Fig. 5Ł) to 65 ± 3 (Fig. 5M) and 180 ± 4 (Fig. 5C) to 72 ± 3 (Fig. 5D), respectively. Therefore, the observed CLM effect in the case of *E. coli* strains (excluding the negative controls, Fig. 5B and L) with Dr fimbriae at the cell surface (IH11128 and BL21(DE3)/pCC90; Fig. 5M and D) is predominantly due to the surface-exposed DraD protein, which induces aggregation of bacterial cells often adjacent to certain parts of HeLa cells (the so-called aggregative adhesion phenotype observed previously, which could represent an adaptation of bacteria to the pathogenic niche) (Zalewska-Piątek et al. 2008). The same effect was visualized in the *E. coli* BL21(DE3)/pCC90DraCmut (Fig. 5H), BL21(DE3)/pCC90D54stop (Fig. 5J), and DR14 strains (Fig. 5O; the average numbers of associated bacteria were 74 ± 3; 76 ± 4; and 64 ± 2, respectively) containing the *dra* gene cluster with the mutated *draC* usher gene or *draE* fimbrial gene. The results obtained were almost the same as in the case of the above-mentioned *E. coli* strains not incubated with CLM (Fig. 5G, I and N).

3.3. Detection of biofilm exopolysaccharides by PAS staining

PAS staining is mainly used for the staining of structures containing carbohydrate molecules. The periodic acid oxidizes the glucose residues and creates aldehydes, which can then react with the Schiff reagent and create a purple-magenta color (Fulcher et al. 2001). PAS staining revealed biofilm formation by the laboratory *E. coli* strains BL21(DE3)/pCC90, BL21(DE3)/pCC90DraDmut, BL21(DE3)/pCC90DraCmut, and BL21(DE3)/pCC90DraD54stop (Fig. 6B, C, D and E) and the clinical *E. coli* strains IH11128 and DR14 (Fig. 6G and H), grown on minimal M63/gluc/LB medium for 24 h in polystyrene plates. The increased exopolysaccharide coverage of the biofilm is represented by the darker purple areas. The strains *E. coli* BL21(DE3) and DR14/*gspD* (Fig. 6A and F), which did not have the ability to form biofilms, were not stained with PAS. In addition, compared to the *E. coli* strains expressing only the DraD protein on the cell surface (DraD$^+$/DraE$^-$; Fig. 6D, E and H), PAS staining was less intense in biofilms formed by *E. coli* strains expressing Dr fimbriae with (DraD$^+$/DraE$^+$; Fig. 6B and G) and without (DraD$^-$/DraE$^+$; Fig. 6C) the DraD tip subunit, suggesting the presence of reduced exopolysaccharide coverage. PAS staining intensity was verified by photogrammetric scanning of the analyzed images (Table 3).

3.4. ATR/FTIR analysis of the chemical properties of the biofilms

FTIR analysis of biofilm formation allowed us to characterize and compare the structures formed by *E. coli* strains expressing extracellular Dr fimbriae with and without the tip subunit (DraD).

The laboratory strains exhibited biofilm formation ability characterized by high protein content. The amide I and amide II bands (1700–1500 cm^{-1}) were clearly visible in the spectra of almost all the recombinant strains (see Fig. 7). The only exception was the BL21(DE3) strain which does not exhibit any significant signs of biofilm formation or cell attachment to the PVC surface. The strain does not carry the *dra* operon genes, therefore it was used as a negative control for biofilm formation (Fig. 7A).

All the spectra presented in Fig. 7, except that of the negative control, share a similar shape pattern in the region of 1200–900 cm^{-1}, which corresponds to the absorption of polysaccharides and phosphates. This implies that the fimbriae (in the case of *E. coli* BL21(DE3)/pCC90 strain; Fig. 7B) or single fimbrial subunits (in the case of *E. coli* BL21(DE3)/pCC90DraDmut, *E. coli* BL21(DE3)/pCC90DraCmut, and *E. coli* BL21(DE3)/pCC90D54stop; Fig. 7C, D, and E) exposed at the surface of a bacterial cell, do not interfere with the metabolism of a cell, allowing the cell to grow and form a stable biofilm. The relative differences in the absorption intensities of individual strains suggest that these strains form biofilms to different extents. In the case of *E. coli* BL21(DE3)/pCC90 and *E. coli* BL21(DE3)/pCC90DraDmut (Fig. 7B and C), which express Dr fimbriae at the cell surface with or without the DraD tip subunit, respectively, the extent of biofilm formation was comparable. The *E. coli* strain BL21(DE3)/pCC90D54stop, which expresses only the DraD protein, exhibited the greatest ability to adhere to the PVC surface (Fig. 7E). Lower adhesion was observed in the case of *E. coli* BL21(DE3)/pCC90DraCmut (Fig. 7D). This strain does not express the DraE subunits of Dr fimbriae (which are accumulated in the periplasm) on the surface of the bacterial cell.

In the case of the clinical strains of *E. coli*, the FTIR spectral intensity differences were smaller (see Fig. 7F and G). However, the chemical composition of the biofilms produced by these strains, which can be characterized using the fingerprinting region of the FTIR spectrum (ca. 1200–900 cm^{-1}), varies to a greater extent than that of the laboratory strains described above. This implies that all the clinical strains possess the same biofilm formation ability. In addition, the *E. coli* IH11128 strain (Fig. 7F) shows a different pattern in the fingerprinting region of the FTIR spectrum, which can be correlated to the expression of other urovirulence factors that cause some changes in the metabolism of the bacterial cell. The higher relative intensity of the FTIR spectrum in amide I (ca. 1650 cm^{-1})

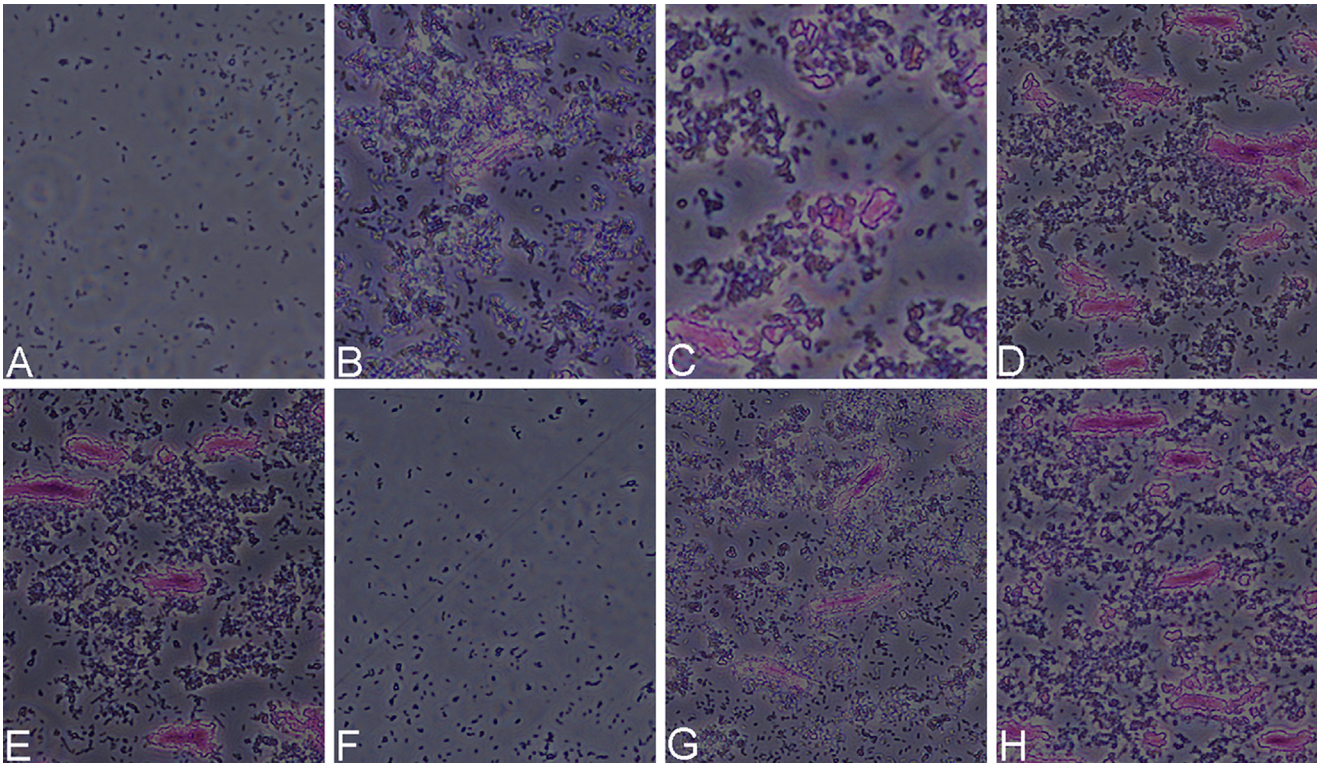

Fig. 6. Determination of exopolysaccharide coverage of *E. coli dra*$^+$ biofilm-forming cells after PAS-staining. Bacterial cells were grown on glass slides and subjected to fixation, PAS-staining, and light microscopy (ME). The images of several biofilms were examined in multiple regions, and representative images are shown. The darker magenta regions represent the increased exopolysaccharide coverage of the biofilm. ME of (A) *E. coli* BL21(DE3), (B) *E. coli* BL21(DE3)/pCC90, (C) *E. coli* BL21(DE3)/pCC90DraDmut, (D) *E. coli* BL21(DE3)/pCC90DraCmut, (E) *E. coli* BL21(DE3)/pCC90D54stop, (F) *E. coli* DR14/*gspD*, (G) *E. coli* IH11128, and (H) *E. coli* DR14. Magnification, 4000× (Olympus CKX41 microscope).

and amide III (ca. 1350–1200 cm^{-1}) regions shows that this strain exhibits a higher protein expression level than the other clinical strains. This ability is crucial for biofilm formation.

4. Discussion

UTI caused by *E. coli* have very serious health and economic impacts on the world (Stamm and Norrby 2001). In the case of bacterial strains that form biofilms, the main problem is the increase in bacterial resistance to applied antibiotic therapy (Gupta et al. 1999; Luzzaro et al. 2006). The combination of ampicillin (β-lactam group of antibiotics) and trimethoprim-sulfametoxazole, used for decades as drugs of choice against UTIs, is usually not sufficient because of the increased resistance of *E. coli* to these antibiotics, which was observed during the 1990s (Gupta et al. 2001). Biofilms, which can usually reach hundreds of microns in depth, are also resistant to disinfectants and many chemical or physical factors (Zottola and Sasahara 1994; Costerton et al. 1995; Kumar and Anand 1998; Kubota et al. 2008).

The aim of the study was to analyze, for the first time, the biochemical properties and some structural elements (such as polysaccharide coverage, proteins, and phosphates) of biofilms formed by uropathogenic *E. coli* strains harboring the *dra* gene cluster. The results obtained can be used as background information in future studies on the development of biofilms by *E. coli dra*$^+$ strains. The major factors associated with the virulence of uropathogenic *E. coli* Dr$^+$ strains are Dr fimbrial adhesin and DraD protein, which is associated with the fimbriae (as the capping subunit) and non-fimbriae-associated form (as the adhesive protein sheath surrounding the bacterial cells). These factors mediate specific attachments to the host receptors or adhesion to abiotic

Table 3
Quantitative analysis of PAS staining intensity of *E. coli dra*$^+$ strains.

E. coli strain	Surface exposure of		PAS staining intensity (OD units)	Distribution of exopolysaccharide coverage
	DraD	DraE		
BL21(DE3)	–	–	0.0	–
BL21(DE)/pCC90	+	+	0.31	[b] rec
BL21(DE3)/pCC90DraDmut	–	+	0.33	[b] rec
BL21(DE3)/pCC90DraCmut	+	–	0.55	[a] iec
BL21(DE3)/pCC90D54stop	+	–	0.58	[a] iec
DR14/*gspD*	–	–	0.0	–
IH11128	+	+	0.3	[b] rec
DR14	+	–	0.53	[a] iec

[a] iec, increased exopolysaccharide coverage.
[b] rec, reduced exopolysaccharide coverage.

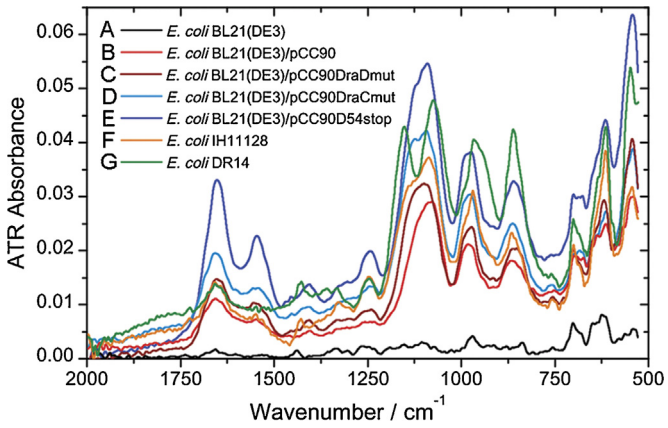

Fig. 7. ATR/FTIR spectra of *E. coli dra*$^+$ strains. Bacterial cells were grown in PVC microtiter plates, purged with PBS, and left to dry at room temperature. The background spectrum of the PVC material was subtracted. (A) *E. coli* BL21(DE3) (black), (B) *E. coli* BL21(DE3)/pCC90 (red), (C) *E. coli* BL21(DE3)/pCC90DraDmut (brown), (D) *E. coli* BL21(DE3)/pCC90DraCmut (light blue), (E) *E. coli* BL21(DE3)/pCC90D54stop (dark blue), (F) *E. coli* IH11128 (orange), and (G) *E. coli* DR14 (green).

surfaces and additionally trigger innate host responses (Zalewska et al. 2005; Zalewska-Piątek et al. 2008, 2009). Therefore, the identification of agents (such as chemical compounds, antibiotics, or pilicides) that might abolish the effect of adherence and prevent biofilm formation by these *E. coli* strains is very important.

We investigated biofilm formation by *E. coli* strains containing the *dra* gene operon and by strains bearing mutations in the *draD* gene (with surface expression of Dr fimbriae) or in the *draE* and *draC* genes (presenting an adhesive sheath composed of only DraD subunits at the cell surface), on an abiotic surface under a range of nutritional factors (glucose, combination of glucose and iron or LB, CAA). We also showed that the high osmotic environment of the medium produced by 1 M sodium chloride affects the ability of the *E. coli dra*$^+$ strains to develop biofilms and their survival, because of its severe growth-inhibitory effect. Conditions typical of the urinary tract include high salt concentrations (400–800 mM NaCl) and low pH (Brauner et al. 1990). Optimal growth of *E. coli* in urine has been observed to occur between pH 6.0 and 7.0 (Shohl and Jannney 1917; Asscher et al. 1966). Therefore, we can apply the obtained results to the biology of uropathogenic *E. coli dra*$^+$ strains within the human urinary tract. An increase in the external osmolarity of the growth medium causes water efflux from the cytoplasm of growing cells therefore, in cells grown at high osmolarity, the amount of cytoplasmic water is less than that in cells grown at lower osmolarity. The loss of water induces active responses in growing cells. This causes alterations in cytoplasmic solutes and turgor pressure. The observed inhibitory effect on biofilm formation by the analyzed *E. coli* strains was strictly related to the osmolarity of sodium chloride, which is double the osmolarity of sucrose at the same molar concentration. However, medium containing 1 M sucrose did not abolish biofilm formation and survival of bacteria, but the biofilm-forming cells displayed thick and filamentous morphology in comparison with bacterial cells grown in medium that was not supplemented with hypertonic sucrose solution. The altered cell morphology might be connected to weakening of the cell wall because of the increased turgor pressure. In addition, in hyper-osmotic sucrose media, the DraD$^+$/DraE$^-$ (pCC90D54stop and pCC90DraCmut) *E. coli* strains also formed cellular clusters (of more than 10 cells in physical contact) of higher density than those formed by the DraD$^+$/DraE$^+$ (pCC90) and DraD$^-$/DraE$^+$ (pCC90DraDmut) *E. coli* strains.

Variants of the DraE protein (JJB30 [T131N], G2152 [I85 M, T131A], G2076 [G68, T88 M], G2099 [D61G, I111T], and G2100 [D52N, D61G]) have been isolated from *E. coli* strains associated with UTI, and they show an increased ability to bind to the DAF receptor at high salt concentrations (800 mM NaCl) relative to the parental DraE (Korotkova et al. 2007). The experiments presented herein may therefore be useful in understanding the mechanism of biofilm development by *E. coli* Dr$^+$ uropathogenic strains in conditions of high osmolarity in the urinary tract.

Further studies were focused on reducing the adhesion step mediated by Dr fimbriae, as the main urovirulence factor of the *E. coli* Dr$^+$ strains, and inhibition of biofilm formation on abiotic surfaces by the studied uropathogens treated with CLM. The results obtained suggest that the first stage of biofilm development requires the synthesis of adhesive proteins (the components of Dr fimbriae and the DraD adhesive sheath) and a coordinated adherence step mediated by Dr haemagglutinin and the DraD protein. The action of CLM is associated with a combination of 2 biological effects: the inhibition of protein synthesis and the inhibition of adherence of Dr haemagglutinin to cell receptors (without affecting the adhesive properties of the DraD protein) (Moazed and Noller 1987; Pettigrew et al. 2009). There are also speculations that CLM may be structurally related to a soluble inhibitor (binding to the hydrophobic pocket I111 and T88 of DraE) associated with the natural environment of *E. coli* strains expressing the Dr family of adhesins (Korotkova et al. 2007). Since adhesion is absolutely required for the process of colonization, blocking adhesion at an early stage can prevent biofilm formation, and thus development of urogenital infections caused by the bacterial strains expressing the parental DraE adhesin. We assume that Dr fimbriae can interact with the abiotic surface in a direct manner. The attachment involves regions of the DraE adhesin that are responsible for non-specific binding to the abiotic surface. The binding of CLM to a region of DraE, involved in interacting with cellular receptors, can change the conformation of the Dr-binding pocket. In a further step, conformational changes in Dr haemagglutinin bound to CLM may mask one of the regions of the Dr fimbrial subunit that is needed to establish a stable attachment to the abiotic surface. In summary, the severe reduction of biofilm development by *E. coli* strains bearing Dr fimbriae (with or without DraD as a capping fimbrial subunit) grown in the presence of CLM confirms the earlier observation that Dr adhesin not bound to CLM is absolutely required to achieve stable cell-to-surface attachment (Zalewska-Piątek et al. 2009). The activity of CLM did not influence the adhesive abilities of the DraD protein, as evidenced by its binding to HeLa cells. However, in the case of *E. coli* strains with only surface-expressed DraD, the presence of CLM also decreased the frequency of the initial cell-to-surface interaction as a result of its conventional bacteriostatic activity associated with the inhibition of protein synthesis. The synthesis of new DraD subunits is necessary to strengthen the interaction with the abiotic surface during the first stage of the biofilm formation.

In further experiments, we showed that bacteria that possess the *dra* gene operon and form biofilm microcolonies are surrounded by a polysaccharide matrix. Exopolysaccharides, a major component of bacterial biofilms, were specifically stained by PAS, confirming the presence of polysaccharides. In addition, PAS staining revealed reduced exopolysaccharide coverage (visible as less intensely stained purple-magenta areas) in *E. coli* strains expressing only cell-surface Dr fimbrial polyadhesins with or without the DraD capping subunit (DraD$^+$/DraE$^+$ and DraD$^-$/DraE$^+$, respectively). The observed effect may be related to the greater ability of *E. coli* DraD$^+$/DraE$^-$ cells to autoaggregate, relative to DraD$^+$/DraE$^+$ and DraD$^-$/DraE$^+$ cells. However, the lower staining intensity does not necessarily mean that the concentration of the individual sugars of the exopolysaccharide matrix is also different.

The exopolysaccharide staining results were in agreement with spectral data from ATR/FTIR spectroscopy (Suci et al. 1997; Schmitt and Flemming 1999; Quilès et al. 2010). ATR/FTIR spectroscopy has

2 important advantages over all staining methods: directness and high discrimination potential. It can directly indicate the presence of adsorbed bacterial cells and the outer matrix (on the basis of the presence or absence of characteristic adsorption bands). ATR/FTIR spectroscopy also provides specific information on the chemical composition of a biofilm and helps to identify pseudo-negative or pseudo-positive results obtained by using staining methods.

Comparable levels of the exopolysaccharide matrix (evidenced by the intensity of the spectra in the region of 1200–900 cm^{-1}) were observed in the case of the laboratory *E. coli* strains BL21(DE3)/pCC90 and BL21(DE3)/pCC90DraDmut and the clinical *E. coli* strain IH11128 that expresses Dr fimbriae at the bacterial cell surface (fimbrial structure with or without the DraD tip subunit, respectively). The highest intensities of exopolysaccharide-related bands were observed in the case of *E. coli* BL21(DE3)/pCC90D54stop and *E. coli* DR14, both expressing only the DraD protein at the surface of bacterial cells; this confirmed the role of proteins with adhesive phenotypes in biofilm formation. The results obtained also showed that the DraD protein alone is sufficient for the initial interaction with the abiotic surface at a higher level than Dr fimbriae with or without the DraD tip subunit. Therefore, we can state that each of these urovirulence factors is able to initiate biofilm formation. The laboratory *E. coli* strain BL21(DE3)/pCC90DraCmut strain, which accumulated Dr fimbrial subunits in the periplasmic space, showed a lower absorbance value than the above bacterial strains. All ATR/FTIR spectra (except the negative control) also displayed bands at approximately 1650 and 1550 cm^{-1} corresponding to proteins (the amide I and amide II bands, respectively). These proteins include not only all proteins expressed by a bacterial cell but also the surface-exposed urovirulence factors, such as the Dr fimbrial subunit and the DraD protein that are responsible for direct cell-to-surface contact. The *E. coli* IH11128 strain showed different spectral patterns in the amide I (ca. 1650 cm^{-1}) and III region (ca. 1350–1200 cm^{-1}) compared to that of the other strains, suggesting the ability of these bacterial cells to express other proteins (possibly also other urovirulence factors besides the DraE and DraD proteins). The preliminary results revealed the ability of the clinical *E. coli* strains IH11128 and DR14 to express (in a phase-variable manner) the surface-located adhesin antigen 43 (Ag43; a member of the autotransporter family) (Henderson et al. 1997; Henderson and Nataro 2001; Anderson et al. 2003), which is associated with urovirulence (data not shown); this might be responsible for the observed differences.

We believe that the data obtained on biofilm-forming cells of *E. coli dra*$^+$ strains and their mutants can contribute to understanding the mechanism of pathogenicity of bacteria colonizing the upper urinary tract. This research will also be helpful in designing alternative therapies for the studied uropathogens, because they demonstrate that blocking the adhesion phenotype of the main urovirulence determinant (Dr fimbriae) of the *E. coli* Dr$^+$ strain is not sufficient to inhibit the initial attachment of bacteria and the subsequent steps of biofilm expansion.

Acknowledgements

This work was supported by the Polish State Committee for Scientific Research, project no. N N401 569438 to B.Z-P and IP2011 041371 (Iuventus Plus) to R.P. We thank Prof. Bogdan Nowicki (Meharry Medical College, Nashville, TN) for supplying the pCC90 and pCC90D54stop plasmids and the *E. coli* DR14 and IH11128 strains.

References

Anderson GG, Palermo JJ, Schilling JD, Roth R, Heuser J, Hultgren SJ. Intracellular bacterial biofilm-like pods in urinary tract infections. Science 2003;301:105–7.
Anderson GG, O'Toole GA. Innate and induced resistance mechanisms of bacterial biofilms. Curr Top Microbiol Immunol 2008;322:85–105.
Arisoy M, Aysev D, Ekim M, Ozel D, Köse SK, Ozso ED, et al. Detection of virulence factors of *Escherichia coli* from children by multiplex polymerase chain reaction. Int J Clin Pract 2006;60:170–3.
Asscher AW, Sussman M, Waters WE, Davis RH, Chick S. Urine as a medium for bacterial growth. Lancet 1966;2:1037–41.
Berger CN, Billker O, Meyer TF, Servin AL, Kansau I. Differential recognition of the carcinoembryonic antigen family by Afa/Dr adhesins of diffusely adhering *Echerichia coli* (Afa/Dr DAEC). Mol Microbiol 2004;52:963–83.
Brauner A, Katouli M, Tullus K, Jacobson SH. Cell surface hydrophobicity, adherence to HeLa cells cultures and haemagglutination pattern of pyelonephritogenic *Escherichia coli* strains. Epidemiol Infect 1990;105:255–63.
Busalmen JP, de Sánchez SR. Influence of pH and ionic strength on adhesion of a wild strain of *Pseudomonas sp*. to titanium. J Ind Microbiol Biotechnol 2001;26:303–8.
Carnoy C, Moseley SL. Mutational analysis of receptor binding mediated by the Dr family of *Escherichia coli* adhesins. Mol Microbiol 1997;23:365–79.
Costerton JW, Lewandowski Z, DeBeer D, Caldwell D, Korber D, James G. Biofilms, the customized microniche. J Bacteriol 1994;176:2137–42.
Costerton JW, Lewandowski Z, Caldwell DE, Korber DR, Lappin-Scott HM. Microbial biofilms. Annu Rev Microbiol 1995;49:711–45.
Costerton JW, Stewart PS, Greenberg EP. Bacterial biofilms: a common cause of persistent infection. Science 1999;284:1318–22.
Danese PN, Pratt LA, Dove SL, Kolter R. The outer membrane protein, antigen 43, mediates cell-to-cell interactions within *Escherichia coli* biofilms. Mol Microbiol 2000;37:424–32.
Emödy L, Kerényi M, Nagy G. Virulence factors of uropathogenic *Escherichia coli*. Int J Antimicrob Agents 2003;2:29–33.
Foxman B. Epidemiology of urinary tract infections: incidence, morbidity, and economic costs. Am J Med 2002;113(Suppl. 1A):S5–13.
Fulcher TP, Dart JK, McLaughlin-Borlace L, Howes R, Matheson M, Cree I. Demonstration of biofilm in infectious crystalline keratopathy using ruthenium red and electron microscopy. Ophthalmology 2001;108:1088–92.
Goluszko P, Moseley SL, Truong LD, Kaul A, Williford JR, Selvarangan R, et al. Development of experimental model of chronic pyelonephritis with *Escherichia coli* O75:K5:H-bearing Dr fimbriae. J Clin Investig 1997;99:1662–72.
Gomez MA, Galvez JM, Hontoria E, González-López J. Influence of ethanol concentration on biofilm bacterial composition from a denitrifying submerged filter used for contaminated groundwater. J Biosci Bioeng 2003;95:245–51.
Guignot J, Hudault S, Kansau I, Chau I, Servin AL. DAF and CEACAMs receptor-mediated internalization and lifestyle of Afa/Dr diffusely adhering *Escherichia coli* into epithelial cells. Infect Immun 2009;77:517–31.
Gupta K, Scholes D, Stamm WE. Increasing prevalence of antimicrobial resistance among uropathogens causing acute uncomplicated cystitis in women. JAMA 1999;281:736–8.
Gupta K, Sahm DF, Mayfield D, Stam WE. Antimicrobial resistance among uropathogens that cause community-acquired urinary tract infections in women: a nation wide analysis. Clin Infect Dis 2001;33:89–94.
Henderson IR, Meehan M, Owen P. A novel regulatory mechanism for a novel phase-variable outer membrane protein of *Escherichia coli*. Adv Exp Med Biol 1997;412:349–55.
Henderson IR, Nataro JP. Virulence functions of autotransporter proteins. Infect Immun 2001;69:1231–43.
Kawarai T, Furukawa S, Narisawa N, Hagiwara C, Ogihara H, Yamasaki M. Biofilm formation by *Escherichia coli* in hypertonic sucrose media. J Biosci Bioeng 2009;107:630–5.
Korotkova N, Cota E, Lebedin Y, Monpouet S, Guignot J, Servin AL, et al. A subfamily of Dr adhesins of *Escherichia coli* bind independently to decay-accelerating factor and the N-domain of carcinoembryonic antigen. J Biol Chem 2006;281:29120–30.
Korotkova N, Chattopadhyay S, Tabata TA, Beskhlebnaya V, Vigdorovich V, Kaiser BK, et al. Selection for functional diversity drives accumulation of point mutations in Dr adhesins of *Escherichia coli*. Mol Microbiol 2007;64:180–94.
Korotkova N, Yarova-Yarovaya Y, Tchesnokova V, Yazvenko N, Carl MA, Stapleton AE, et al. *Escherichia coli* DraE adhesin-associated bacterial internalization by epithelial cells is promoted independently by decay-accelerating factor and carcinoembryonic antigen-related cell adhesion molecule binding and does not require the DraD invasin. Infect Immun 2008a;76:3869–80.
Korotkova N, Yang Y, Le Trong I, Cota E, Demeler B, Marchant J, et al. Binding of Dr adhesins of *Escherichia coli* to carcinoembryonic antigen triggers receptor dissociation. Mol Microbiol 2008b;67:420–34.
Kubota H, Senda S, Nomura N, Tokuda H, Uchiyama H. Biofilm formation by lactic acid bacteria and resistance to environmental stress. J Biosci Bioeng 2008;106:381–6.
Kumar CG, Anand SK. Significance of microbial biofilms in food industry: a review. Int J Food Microbiol 1998;42:9–27.
Le Bouguénec C, Servin AL. Diffusely adherent *Escherichia coli* strains expressing Afa/Dr adhesins (Afa/Dr DAEC): hitherto unrecognized pathogens. FEMS Microbiol Lett 2006;256:185–94.
Luzzaro F, Mezzatesta M, Mugnaioli C, Perilli M, Stefani S, Amicosante G, et al. Trends in production of extended-spectrum beta-lactamases among enterobacteria of medical interest: report of the second Italian nationwide survey. J Clin Microbiol 2006;44:1659–64.
Medof ME, Walter EI, Rutgers JL, Knowles DM, Nussenzweig V. Identification of the complement decay-accelerating factor (DAF) on epithelium and glandular cells and in body fluids. J Exp Med 1987;165:848–68.

Moazed D, Noller HF. Chloramphenicol, erythromycin, carbomycin and vernamycin B protect overlapping sites in the peptidyl transferase region of 23S ribosomal RNA. Biochimie 1987;69:879–84.
Nowicki B, Barrish JP, Korhonen T, Hull RA, Hull SI. Molecular cloning of the *Escherichia coli* O75X adhesin. Infect Immun 1987;55:3168–73.
Nowicki B, Moulds J, Hull R, Hull S. A haemagglutinin of uropathogenic *Escherichia coli* recognizes the Dr blood group antigen. Infect Immun 1988;56:1057–60.
Nowicki B, Svanborg-Eden C, Hull R, Hull S. Molecular analysis and epidemiology of the Dr haemagglutinin of uropathogenic *Escherichia coli*. Infect Immun 1989;57:446–51.
Nowicki B, Selvarangan R, Nowicki S. Family of *Escherichia coli* Dr adhesins: decay-accelerating factor receptor recognition and invasiveness. J Infect Dis 2001;183(Suppl. 1):S24–7.
Oelschlaeger TA, Dobrindt U, Hacker J. Pathogenicity islands of uropathogenic *E. coli* and the evolution of virulence. Int J Antimicrob Agents 2002;19:517–21.
Pettigrew DM, Roversi P, Davies SG, Russell AJ, Lea SM. A structural study of the interaction between the Dr haemagglutinin DraE and derivatives of chloramphenicol. Acta Crystallogr D Biol Crystallogr 2009;65:513–22.
Prigent-Combaret C, Brombacher E, Vidal O, Ambert A, Lejeune P, Landini P, et al. Complex regulatory network controls initial adhesion and biofilm formation in *Escherichia coli* via regulation of the *csgD* gene. J Bacteriol 2001;183: 7213–23.
Quilès F, Humbert F, Delille A. Analysis of changes in attenuated total reflection FTIR fingerprints of *Pseudomonas fluorescens* from planktonic state to nascent biofilm state. Spectrochim Acta A 2010;75:610–6.
Record Jr MT, Courtenay ES, Cayley DS, Gutman HJ. Responses of *E. coli* to osmotic stress: large changes in amounts of cytoplasmic solutes and water. Trends Biochem Sci 1998;23:143–8.
Schmitt J, Flemming HC. Water binding in biofilms. Water Sci Tech 1999;39:77–82.
Servin AL. Pathogenesis of Afa/Dr diffusely adhering *Escherichia coli*. Clin Microbiol Rev 2005;18:264–92.
Shohl AT, Jannney JH. Optimal growth of *Escherichia coli* in urine varying hydrogen ion concentrations. J Urol 1917;1:2111–228.
Soto SM, Smithson A, Martinez JA, Horcajada JP, Mensa J, Vila J. Biofilm formation in uropathogenic *Escherichia coli* strains: relationship with prostatitis, urovirulence factors and antimicrobial resistance. J Urol 2007;177:365–8.
Stamm WE, Norrby SR. Urinary tract infections: disease panorama and challenges. J Infect Dis 2001;183(Suppl 1):S1–4.
Stewart PS, Franklin MJ. Physiological heterogeneity in biofilms. Nat Rev Microbiol 2008;6:199–210.
Suci PA, Siedlecki KJ, Palmer Jr RJ, White DC, Geesey GG. Combined light microscopy and attenuated total reflection Fourier transform infrared spectroscopy for integration of biofilm structure, distribution, and chemistry at solid-liquid interfaces. Appl Environ Microbiol 1997;63:4600–3.
Terada A, Hibiya K, Nagai J, Tsuneda S, Hirat A. Nitrogen removal characteristics and biofilm analysis of a membrane-aerated biofilm reactor applicable to high-strength nitrogenous wastewater treatment. J Biosci Bioeng 2003;95: 170–8.
Van Loy C, Sokurenko EV, Moseley SL. The major structural subunits of Dr and F1845 fimbriae are adhesins. Infect Immun 2002a;70:1694–702.
Van Loy C, Sokurenko EV, Samudrala R, Moseley SL. Identification of amino acids in the Dr adhesin required for binding to decay-accelerating factor. Mol Microbiol 2002b;45:439–52.
Westerlund B, Kuusela P, Risteli J, Risteli L, Vartio T, Rauvala H, et al. The O75X adhesin of uropathogenic *Escherichia coli* is a type IV collagen-binding protein. Mol Microbiol 1989;3:329–37.
Wimpenny JWT, Colasanti R. A unifying hypothesis for the structure of microbial biofilms based on cellular automaton models. FEMS Microbiol Ecol 1997;22:1–16.
Yamamoto S. Molecular epidemiology of uropathogenic *Escherichia coli*. J Infect Chemother 2007;13:68–73.
Zalewska B, Piątek R, Bury K, Samet B, Nowicki BJ, Nowicki S, et al. A surface-exposed DraD protein of uropathogenic *Escherichia coli* bearing Dr fimbriae may be expressed and secreted independently from DraC usher and DraE adhesin. Microbiology 2005;151:2477–86.
Zalewska-Piątek B, Bury K, Piątek R, Bruździak P, Kur J, Type II. secretory pathway for surface secretion of DraD invasin from the uropathogenic *Escherichia coli* Dr^+ strain. J Bacteriol 2008;190:5044–56.
Zalewska-Piątek BM, Wilkanowicz SI, Piątek RJ, Kur JW. Biofilm formation as a virulence determinant of uropathogenic *Escherichia coli* Dr^+ strains. Pol J Microbiol 2009;58:223–9.
Zottola EA, Sasahara KC. Microbial biofilms in the food processing industry-should they be a concern? Int J Food Microbiol 1994;23:125–48.